Published in final edited form as:
J Dent Res. 2008 May ; 87(5): 451–455.

Reduced Amelogenin-MMP20 Interactions in Amelogenesis Imperfecta

K. Tanimoto[1], **T. Le**[1], **L. Zhu**[1], **H.E. Witkowska**[2], **S. Robinson**[2], **S. Hall**[2], **P. Hwang**[3], **P. DenBesten**[1], and **W. Li**[1,*]

[1]Department of Orofacial Sciences, School of Dentistry, University of California at San Francisco, 513 Parnassus Avenue, San Francisco, CA 94143, USA

[2]Department of Cell and Tissue Biology, School of Dentistry, University of California at San Francisco, 513 Parnassus Avenue, San Francisco, CA 94143, USA

[3]Department of Biochemistry and Biophysics, School of Medicine, University of California at San Francisco, CA, USA

Abstract

Amelogenin with a proline 41 to threonine mutation (P41T) is hydrolyzed at a lower rate by matrix metalloproteinase 20 (MMP20), resulting in an inherited tooth enamel defect, amelogenesis imperfecta (AI). The aim of this study was to elucidate the effect of P41T on the interactions between amelogenin and MMP20, which may contribute to the formation of this type of AI. The interactions of a recombinant wild-type human amelogenin and its P41T mutant with recombinant human MMP20 were compared by substrate competition assay, pull-down assay, and surface plasmon resonance (SPR). The results showed that the binding of the P41T mutant amelogenin for MMP20 was significantly lower than that of wild-type amelogenin. Our study supports a model in which the P41T mutation reduces the interactions between amelogenin and MMP20, leading to decreased degradation of amelogenin by MMP20, and resulting in AI.

Keywords

amelogenin; matrix metalloproteinase 20; protein interaction; tooth enamel; biomineralization; amelogenesis imperfecta

INTRODUCTION

Tooth enamel, which is composed of well-organized hydroxyapatite (HAP) crystals, is the hardest tissue in vertebrate animals. Biomineralized enamel develops from tooth enamel extracellular matrix proteins secreted by epithelially derived ameloblasts. Formation of enamel is a dynamic process involving protein-crystal and protein-proteinase interactions, in which the proteins in the enamel matrix are removed by proteinases, thus allowing the HAP crystals to elongate; ultimately, HAP makes up greater than 95% of the tooth enamel (Robinson *et al.*, 1997; Smith, 1998; Fincham *et al.*, 1999).

The primary protein components of the secreted enamel matrix are amelogenins and their hydrolytic products. Amelogenins are synthesized from alternatively spliced mRNAs, ranging in size from 5 to 28 kDa (Lau *et al.*, 1992; Li *et al.*, 1995; Hu *et al.*, 1996a,b). These

*corresponding author, Wu.Li@ucsf.edu.

A supplemental appendix to this article is published electronically only at http://jdr.iadrjournals.org/cgi/content/full/87/5/451/DC1.

proteins are further processed at both their C- and N-termini by matrix metalloproteinase 20 (MMP20), to form many smaller peptide fragments, including a 23-kDa amelogenin (Amg23), a 5-kDa tyrosine-rich amelogenin peptide (TRAP), and a 5.4-kDa leucine-rich amelogenin peptide (LRAP). The Amg23 and TRAP are formed from a full-length amelogenin (Amg25), while the LRAP is generated from an alternatively spliced LRAP precursor (Fincham *et al.*, 1981; Gibson *et al.*, 1991; Fincham and Moradian-Oldak, 1993, 1995; Moradian-Oldak *et al.*, 1994). These protein fragments may play important roles in the formation and elongation of tooth enamel crystals.

A transversion mutation of cytosine to adenine in exon 6 of the X-chromosomal amelogenin gene, resulting in a proline-to-threonine substitution at residue 41 (P41T) in the amelogenin protein, has been reported (Collier *et al.*, 1997). This gives rise to the clinical condition amelogenesis imperfecta (AI). Persons with AI have been reported to show a hypomature phenotype, characterized by hypomineralized enamel matrix, with more proteins retained and fewer minerals formed in the enamel matrix (Collier *et al.*, 1997; Ravassipour *et al.*, 2000; Hart *et al.*, 2002). We have reported that MMP20 cleaves amelogenin between Trp45 and Leu46, to form TRAP (Li *et al.*, 1999). The P41T mutation does not alter the cleavage site at T45/L46, but reduces the rate of hydrolysis of amelogenin, resulting in decreased TRAP formation (Li *et al.*, 2001, 2003). Our previous studies also showed that the P41T mutation alters the enzyme kinetics of MMP20 on its amelogenin substrate (Li *et al.*, 2001, 2003), but the mechanism of the impairment caused by this mutation is still unclear.

We hypothesized that the P41T point mutation affects the binding affinity between amelogenin and MMP20, resulting in decreased substrate degradation. In this study, we used different methods to analyze the amelogenin-MMP20 interactions, including a state-of-the-art technique, surface plasmon resonance (SPR), for our quantitative and dynamic experiments. For these protein-protein interaction assays, we used an intact and inactive MMP20 protein, which was created by introducing a point mutation, Glu225 to Ala, in its catalytic domain, to prevent interference from the smaller fragments produced by autolysis of this protein during its expression and purification, and when the enzyme was being used to degrade its substrates (Li *et al.*, 1999; Wang *et al.*, 2006). The results of this study provide new insights into the pathogenesis of AI, and are also helpful in our understanding of the interactions between amelogenin and MMP20 during tooth enamel formation.

MATERIALS & METHODS

Purification and Characterization of Amelogenins, Wild-type Active Recombinant Human MMP20 (rhMMP20), and Mutated Inactive rhMMP20

Both wild-type amelogenin (rh174) and P41T mutant amelogenin (P41T) were expressed and purified as described previously (Li *et al.*, 2001, 2003). The wild-type recombinant active human MMP20 (rhMMP20) used in this study was expressed and purified according to a previously described protocol for recombinant bovine MMP20 (Li *et al.*, 1999).

To create an inactive rhMMP20 for the protein-protein interaction studies, we introduced a point mutation into the rhMMP20 expression construct, resulting in a substitution of Glu at position 227 for Ala (E227A). This was done with the use of a QuikChange XL site-directed mutagenesis kit (Stratagene, La Jolla, CA, USA) and the following primers: 5′-GTT GCT GCT CAT GCA TTT GGC CAT GCC-3′ and 5′-GGC ATG GCC AAA TGC ATG AGC AGC AAC-′. Expression, purification, and refolding of the E227A inactive enzyme were performed in parallel with wild-type rhMMP20, by the same protocol. Both rhMMP20 and E227A inactive rhMMP20 were characterized by SDS-PAGE and Western blot analysis. Enzymatic activities of the purified proteases were analyzed by zymography and quenched-

peptide assay (Li *et al.*, 1999; Wang *et al.*, 2006). The digested amelogenins were visualized by SDS-PAGE and analyzed by MALDI-TOF mass spectrometry (MS).

Peptide Competition Assay for Comparison of the Binding Affinities of Active rhMMP20 for Wild-type and P41T Mutant Amelogenin Peptides

We designed a competition assay to measure the effect of the P41T mutation of amelogenin on its binding affinity for active MMP20. Two peptides—A1 (SYGYEPMGGWLHHQ), which corresponds to amino acid residues 36–49 of the wild-type human amelogenin sequence, and M1 (SYGYETMGGWLHHQ), which has the same sequence as A1, except for a single substitution mutation (underlined) corresponding to residue 41 of the full-length amelogenin (Collier *et al.*, 1997)—were synthesized (Genemed, South San Francisco, CA, USA).

Both A1 and M1 peptides were dissolved at a concentration of 10 μM in assay buffer (50 mM Tris-HCl at pH 7.5, 10 mM $CaCl_2$, 50 μM $ZnCl_2$, and 150 mM NaCl) containing 5 μM of fluorescent quenched-peptide Mca-KPLGL-Dpa-AR-NH_2 (M2350, Bachem Biosciences, King of Prussia, PA, USA). Active rhMMP20 was added to the reaction buffer to a final concentration of 40 nM. All groups were assayed in triplicate, and the fluorescence intensity of the enzymatic products was monitored by means of a fluorometer (Molecular Devices, Sunnyvale, CA, USA). The digested products were identified by MALDI-TOF MS.

Surface Plasmon Resonance Analysis of the Binding of E227A rhMMP20 for Different Amelogenins (rh174 and P41T Mutant)

The binding affinity of rh174 or P41T amelogenin for E227A rhMMP20 was analyzed by SPR with the use of a Biacore 1000 optical biosensor (GE Healthcare, Piscataway, NJ, USA). Briefly, N-terminally His-tagged E227A rhMMP20 at a concentration of 0.5 mM was immobilized on a nitrilotriacetic acid (NTA) sensor chip pre-activated with 0.5 mM Ni^{2+} (Huang *et al.*, 2006). After the sample was washed, rh174 or P41T amelogenin at various concentrations (0.2, 0.5, and 1 mM) was injected over the immobilized E227A rhMMP20 surface for 80 sec at a flow rate of 15 μL/min. An NTA sensor flow channel without rhMMP20 was used as a subtractive reference control for non-specific binding of amelogenins to the chip surface. All binding experiments were performed in a running buffer of 10 mM HEPES at pH 6.8, 0.01% Tween-20, 0.5% BSA, and 300 mM NaCl, at 25°C. The NTA surface was regenerated by injection of 20 μL 0.25% SDS, followed by injection of 15 μL of 0.35 M EDTA at a flow rate of 15 μL/min. The association, dissociation, and regeneration phases were monitored by measurement of SPR resonance units (RU) over time (sec). The sensorgrams were analyzed by BIAevaluation Software (GE Healthcare) and a 1:1 (mol/mol) Langmuir binding model for the determination of rate constants. The 1:1 Langmuir binding model represents a simple reversible interaction between 2 molecules. The values of the association rate (K_{on}) and the dissociation rate (K_{off}) between an analyte and a ligand were calculated from the forward and reverse reactions of the optimal fitted binding curves, respectively. The association constant (K_a) was obtained as a ratio of K_{on}/K_{off}. The K_{on}, K_{off}, and K_a values of E227A rhMMP20 binding to rh174 or P41T amelogenin were compared. All analyses were run in triplicate, with the same conditions used for determination of the average and standard deviation values.

Statistical Analysis

The data collected from the pull-down assays and SPR studies were analyzed by Student's *t* test with Graphpad Prism 4.0a software (Graphpad Software, Inc., San Diego, CA, USA). The data from the peptide competition assays were analyzed by one-way ANOVA, followed by Scheffé's *post hoc* test.

RESULTS

Purification and Characterization of E227A rhMMP20

After refolding and activation by stepwise dialysis, wild-type rhMMP20 underwent autolysis into multiple smaller fragments, as revealed by SDS-PAGE (Fig. 1A), zymography (data not shown), and Western blot (data not shown), with predominant active autolytic bands at 25 and 21 kDa. After refolding, the major band of E227A rhMMP20 remained as an intact 55-kDa protein (Fig. 1A).

The quenched-peptide assay and zymography showed that wild-type rhMMP20 was active, whereas the E227A MMP20 was completely inactive (Fig. 1B). After incubation of active rhMMP20 or inactive E227A rhMMP20 with rh174 amelogenin for 5 hrs, only active rhMMP20 was able to digest the amelogenin (Fig. 1C).

Competition Assays to Compare the Binding of Active rhMMP20 for Amelogenin Peptides

The fluorescent intensity observed in a competition assay is directly related to the amount of digested quenched peptides. This fluorescent signal is inversely related to the affinity of active rhMMP20 for either unmodified peptide A1 or mutant M1, which act as competitors of the quenched peptide for MMP20 binding. The highest relative fluorescence units (RFU) were observed in the control reaction consisting of MMP20 and quenched peptide without competitors (Fig. 2). The slope of the curve of RFU values obtained from a digestion reaction containing MMP20, quenched peptide, and the mutated peptide M1 (11.1 ± 0.6) was significantly higher than that for the peptide A1 (8.3 ± 0.5) ($n = 3$, $p < 0.01$) (Fig. 2), suggesting that peptide M1 has a lower binding affinity than A1 for rhMMP20.

Surface Plasmon Resonance Comparison of the Binding Affinity of Amelogenins for E227A rhMMP20

The binding of immobilized E227A rhMMP20 for different concentrations (0.2, 0.5, and 1 μM) of rh174 and P41T amelogenins were analyzed by SPR, and the reference-subtracted averaged data are presented in sensorgrams (Fig. 3). The response level after 80 sec from the binding of rh174 amelogenin for E227A rhMMP20 (left panel in Fig. 3) was consistently higher than that of the P41T mutant at similar concentrations (right panel in Fig. 3), suggesting that rh174 amelogenin has greater binding affinity for E227A rhMMP20 than does P41T mutant amelogenin. Kinetic data showed that the average value of the on-rate constant, K_{on}, of rh174 amelogenin binding for E227A rhMMP-20 ($6.45 \times 10^4 \pm 2.46 \times 10^4$ $M^{-1}s^{-1}$) was significantly higher than that of the P41T mutant ($1.87 \times 10^4 \pm 0.70 \times 10^4$ $M^{-1}s^{-1}$) ($p < 0.05$, Table). However, there was no significant difference in the average values of the off-rate constant, K_{off}, between rh174 and P41T amelogenin ($p > 0.05$, Table). The difference in association constants indicates that rh174 amelogenin binds for E227A rhMMP-20 at higher affinity than does the P41T mutant. The affinity constant ($K_a = K_{on}/K_{off}$) of rh174 amelogenin binding for E227A rhMMP20 was determined to be $1.19 \times 10^7 \pm 0.57 \times 10^7$ M^{-1}, three times higher than that of the P41T mutant binding for E227A rhMMP20 ($3.23 \times 10^6 \pm 1.31 \times 10^6$ M^{-1}) ($p < 0.05$, Table).

DISCUSSION

A proline-41 to threonine (P41T) mutation in amelogenin leads to disrupted tooth enamel mineralization and results in AI (Collier *et al.*, 1997). How can a single proline substitution produce such a significant alteration in enamel maturation and mineralization? One possible explanation is that the mutated amelogenin generates more heterogeneous assemblies than does wild-type amelogenin, which alters crystal formation (Moradian-Oldak *et al.*, 2000; Moradian-Oldak, 2001). However, as shown in our previous studies (Li *et al.*, 2001, 2003),

another possibility is that the P41T mutation makes amelogenin a less favorable substrate for MMP20, resulting in decreased degradation of amelogenins from the matrix. This decreased degradation may be the result of impaired interactions between these 2 proteins caused by the proline 41 mutation. Proline residues have been reported to be critical in protein-protein recognition (Kay *et al.*, 2000). In this study, we used different assays—including competition assay, pull-down assay (APPENDIX), and SPR—to investigate the protein-protein interactions of MMP20 with the wild-type amelogenin and the P41T mutant. We directly confirmed that a single proline mutation at the N-terminus of amelogenin could dramatically affect the interactions between these 2 proteins.

The E227A mutation was introduced into the catalytic domain of MMP20 to create an inactive proteinase, which keeps the proteinase intact and minimizes the interference from the autolytic products of MMP20, but without affecting its substrate binding. The same strategy has been used to mutate Glu200 to Ala in MMP1 to inactivate the enzyme, while still keeping its binding affinity for its collagen substrate (Chung *et al.*, 2004). Analysis of our enzyme activity assay data indicated that MMP20 was successfully inactivated by this mutation, while preserving its binding affinity for amelogenins, as shown in the competition and pull-down assays (see APPENDIX), and the SPR analysis. This is crucial for our studies to observe the protein interactions between MMP20 and amelogenin.

In the present SPR study, the kinetics parameters (K_{on}, K_{off}, and K_a) of wild-type rh174 amelogenin binding for E227A rhMMP20 were 6.45×10^4 M^{-1} s^{-1}, 5.68×10^{-3} s^{-1}, and 1.19×10^7 M^{-1}, respectively. The K_a value represents a high-affinity interaction between MMP20 and rh174 amelogenin. In a previous study (Roeb *et al.*, 2002), investigators demonstrated that K_{on} and K_{off} of recombinant MMP9 binding for its substrate were 3.83×10^5 M^{-1} s^{-1} and 1.01×10^{-2} s^{-1} by means of SPR analysis. The dissociation constant (K_d) was 12 nM, which can be converted to a K_a value of 3.79×10^7 M^{-1}, suggesting a level of affinity between enzyme and substrate similar to that observed in our rhMMP20/rh174 amelogenin interaction study. The similarity of the results may not be surprising, since there is high homology between different MMP sequences, especially in the catalytic domains (Massova *et al.*, 1998).

The impaired amelogenin-MMP20 interaction caused by mutation of a single residue is related to the unique structure of proline. Proline has a pyrolidine five-membered ring in its structure, which blocks free rotation about the N-C bond. Thus, proline reduces the structural flexibility of the peptide backbone and holds the following amino group in a rigid conformation (Fleminger and Yaron, 1983; Yaron, 1987; Yaron and Naider, 1993). In amelogenin, the proline residue upstream to the MMP20 cleavage site may be part of a docking site for MMP20 to bind (Turk *et al.*, 2006), or it may aid in positioning the cleavage-site residues into the enzyme's active site; indeed, there is a proline residue in the upstream sequence of every MMP20 cleavage site in amelogenin. Mutation of the critical proline will decrease the binding affinity of amelogenin for proteinases, thus impairing downstream proteolytic cleavage.

In conclusion, using the complementary techniques of pull-down assay, competition assay, and SPR analysis, we tested the binding kinetics of amelogenins and MMP20. We found that the P41T mutation of amelogenin reduces its binding affinity for MMP20. The reduced proteinase-substrate interactions may contribute to the delayed removal of amelogenin from the developing enamel matrix and give rise to AI.

Supplementary Material

Refer to Web version on PubMed Central for supplementary material.

Acknowledgments

This research was supported by R01-DE13508 and R01-DE015821 from the National Institute of Dental and Craniofacial Research. MS analysis was performed at the UCSF Mass Spectrometry Facility, funded by the Sandler Family Foundation grant.

References

Chung L, Dinakarpandian D, Yoshida N, Lauer-Fields JL, Fields GB, Visse R, et al. Collagenase unwinds triple-helical collagen prior to peptide bond hydrolysis. EMBO J. 2004; 23:3020–3030. [PubMed: 15257288]

Collier PM, Sauk JJ, Rosenbloom SJ, Yuan ZA, Gibson CW. An amelogenin gene defect associated with human X-linked amelogenesis imperfecta. Arch Oral Biol. 1997; 42:235–242. [PubMed: 9188994]

Fincham AG, Moradian-Oldak J. Amelogenin post-translational modifications: carboxy-terminal processing and the phosphorylation of bovine and porcine “TRAP” and “LRAP” amelogenins. Biochem Biophys Res Commun. 1993; 197:248–255. [PubMed: 8250931]

Fincham AG, Moradian-Oldak J. Recent advances in amelogenin biochemistry. Connect Tissue Res. 1995; 32:119–124. [PubMed: 7554907]

Fincham AG, Belcourt AB, Termine JD, Butler WT, Cothran WC. Dental enamel matrix: sequences of two amelogenin polypeptides. Biosci Rep. 1981; 1:771–778. [PubMed: 7306685]

Fincham AG, Moradian-Oldak J, Simmer JP. The structural biology of the developing dental enamel matrix. J Struct Biol. 1999; 126:270–299. [PubMed: 10441532]

Fleminger G, Yaron A. Sequential hydrolysis of proline-containing peptides with immobilized aminopeptidases. Biochim Biophys Acta. 1983; 743:437–446. [PubMed: 6830820]

Gibson CW, Golub E, Ding WD, Shimokawa H, Young M, Termine J, et al. Identification of the leucine-rich amelogenin peptide (LRAP) as the translation product of an alternatively spliced transcript. Biochem Biophys Res Commun. 1991; 174:1306–1312. [PubMed: 1996994]

Hart PS, Aldred MJ, Crawford PJ, Wright NJ, Hart TC, Wright JT. Amelogenesis imperfecta phenotype-genotype correlations with two amelogenin gene mutations. Arch Oral Biol. 2002; 47:261–265. [PubMed: 11922869]

Hu CC, Zhang C, Qian Q, Ryu OH, Moradian-Oldak J, Fincham AG, et al. Cloning, DNA sequence, and alternative splicing of opossum amelogenin mRNAs. J Dent Res. 1996a; 75:1728–1734. [PubMed: 8955666]

Hu CC, Bartlett JD, Zhang CH, Qian Q, Ryu OH, Simmer JP. Cloning, cDNA sequence, and alternative splicing of porcine amelogenin mRNAs. J Dent Res. 1996b; 75:1735–1741. [PubMed: 8955667]

Huang Z, Park JI, Watson DS, Hwang P, Szoka FC Jr. Facile synthesis of multivalent nitrilotriacetic acid (NTA) and NTA conjugates for analytical and drug delivery applications. Bioconjug Chem. 2006; 17:1592–1600. [PubMed: 17105240]

Kay BK, Williamson MP, Sudol M. The importance of being proline: the interaction of proline-rich motifs in signaling proteins with their cognate domains. FASEB J. 2000; 14:231–241. [PubMed: 10657980]

Lau EC, Simmer JP, Bringas P Jr, Hsu DD, Hu CC, Zeichner-David M, et al. Alternative splicing of the mouse amelogenin primary RNA transcript contributes to amelogenin heterogeneity. Biochem Biophys Res Commun. 1992; 188:1253–1260. [PubMed: 1445358]

Li R, Li W, DenBesten PK. Alternative splicing of amelogenin mRNA from rat incisor ameloblasts. J Dent Res. 1995; 74:1880–1885. [PubMed: 8600184]

Li W, Machule D, Gao C, DenBesten PK. Activation of recombinant bovine matrix metalloproteinase-20 and its hydrolysis of two amelogenin oligopeptides. Eur J Oral Sci. 1999; 107:352–359. [PubMed: 10515200]

Li W, Gibson CW, Abrams WR, Andrews DW, DenBesten PK. Reduced hydrolysis of amelogenin may result in X-linked amelogenesis imperfecta. Matrix Biol. 2001; 19:755–760. [PubMed: 11223334]

Li W, Gao C, Yan Y, DenBesten P. X-linked amelogenesis imperfecta may result from decreased formation of tyrosine rich amelogenin peptide (TRAP). Arch Oral Biol. 2003; 48:177–183. [PubMed: 12648554]

Massova I, Kotra LP, Fridman R, Mobashery S. Matrix metalloproteinases: tructures, evolution, and diversification. FASEB J. 1998; 12:1075–1095. [PubMed: 9737711]

Moradian-Oldak J. Amelogenins: assembly, processing and control of crystal morphology. Matrix Biol. 2001; 20:293–305. [PubMed: 11566263]

Moradian-Oldak J, Simmer JP, Sarte PE, Zeichner-David M, Fincham AG. Specific cleavage of a recombinant murine amelogenin at the carboxy-terminal region by a proteinase fraction isolated from developing bovine tooth enamel. Arch Oral Biol. 1994; 39:647–656. [PubMed: 7980113]

Moradian-Oldak J, Paine ML, Lei YP, Fincham AG, Snead ML. Self-assembly properties of recombinant engineered amelogenin proteins analyzed by dynamic light scattering and atomic force microscopy. J Struct Biol. 2000; 131:27–37. [PubMed: 10945967]

Ravassipour DB, Hart PS, Hart TC, Ritter AV, Yamauchi M, Gibson C, et al. Unique enamel phenotype associated with amelogenin gene (AMELX) codon 41 point mutation. J Dent Res. 2000; 79:1476–1481. [PubMed: 11005731]

Robinson C, Brookes SJ, Bonass WA, Shore RC, Kirkham J. Enamel maturation. Ciba Found Symp. 1997; 205:156–170. [PubMed: 9189623]

Roeb E, Schleinkofer K, Kernebeck T, Potsch S, Jansen B, Behrmann I, et al. The matrix metalloproteinase 9 (mmp-9) hemopexin domain is a novel gelatin binding domain and acts as an antagonist. J Biol Chem. 2002; 277:50326–50332. [PubMed: 12384502]

Smith CE. Cellular and chemical events during enamel maturation. Crit Rev Oral Biol Med. 1998; 9:128–161. [PubMed: 9603233]

Turk BE, Lee DH, Yamakoshi Y, Klingenhoff A, Reichenberger E, Wright JT, et al. MMP-20 is predominately a tooth-specific enzyme with a deep catalytic pocket that hydrolyzes type V collagen. Biochemistry. 2006; 45:3863–3874. [PubMed: 16548514]

Wang S, Zhu J, Zhang Y, Li L, DenBesten P, Li W. On-column activation of bovine recombinant metalloproteinase 20. Anal Biochem. 2006; 356:291–293. [PubMed: 16890905]

Yaron A. The role of proline in the proteolytic regulation of biologically active peptides. Biopolymers. 1987; 26(Suppl):215–222.

Yaron A, Naider F. Proline-dependent structural and biological properties of peptides and proteins. Crit Rev Biochem Mol Biol. 1993; 28:31–81. [PubMed: 8444042]

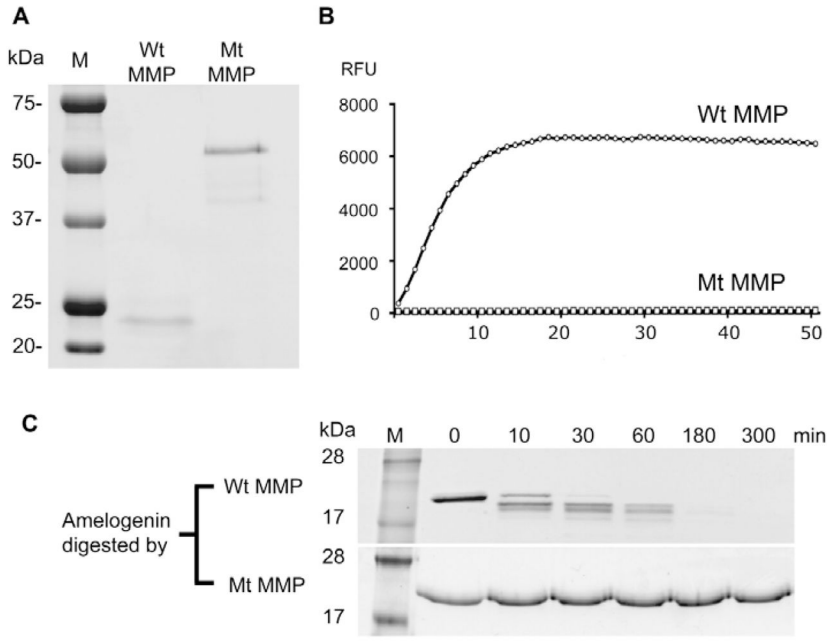

Figure 1.

Characterizations of inactive E227A mutated rhMMP20. **(A)** SDS-PAGE analysis of rhMMP20s after purification showed that the 55-kDa intact protein of wild-type active rhMMP20 (left lane) was absent; however, the autolytic products of rhMMP20 were predominantly located at 25 and 21 kDa. A predominant 55-kDa band with minor smaller fragments of inactive E227A rhMMP20 can be seen in the right lane of the SDS-PAGE gel. M, protein standard; Wt MMP, active wild-type rhMMP20; Mt MMP, inactive E227A rhMMP20. **(B)** Quenched-peptide digestion assay showed that wild-type rhMMP20 (Wt MMP20) was active. However, the enzymatic activity of inactive E227A rhMMP20 (Mt MMP20) was undetectable. The RFU readings depended on the amount of fluorophores released from the quencher in the quenched peptide by rhMMP20 hydrolysis. RFU, relative fluorescence units. **(C)** SDS-PAGE analysis showed that the wild-type human recombinant amelogenin is digested by wild-type active rhMMP20 (Wt MMP20, upper row), but is not degraded by mutated inactive E227A rhMMP20 (Mt MMP, lower row).

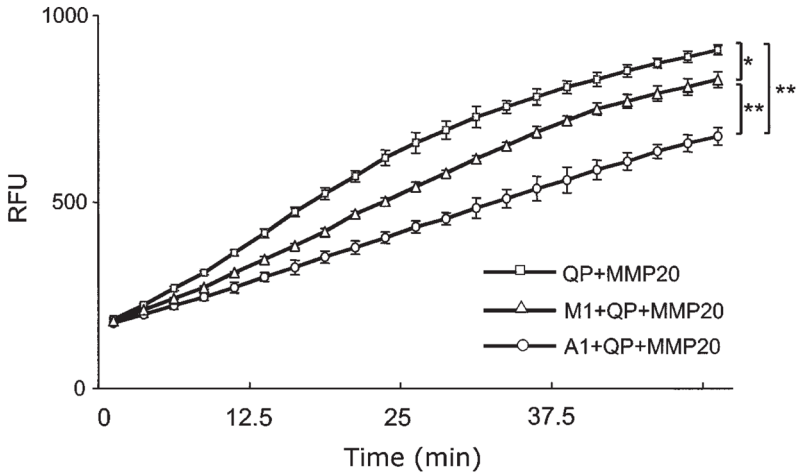

Figure 2.

Comparison of the binding affinities of active rhMMP20 for amelogenin peptides by peptide competition assays. The fluorescence intensity observed in a peptide competition assay was directly related to the amount of digested quenched peptides. Therefore, the fluorescent signal was inversely related to the affinity of active rhMMP20 for the competitor peptides (A1 or M1), which competed with the quenched peptide for binding to MMP20. The reaction without any competitors (QP+MMP20) had the highest RFU readings (curve's slope = 12.34 ± 0.31, n = 3). The wild-type A1 peptide (A1+QP+MMP20) is a significantly stronger competitor (curve's slope = 8.29 ± 0.46, n = 3) than M1 peptide (M1+QP +MMP20), containing a P-to-T mutation (curve's slope = 11.14 ± 0.64, n = 3). QP, quenched peptide; A1, peptide without mutation; M1, peptide with mutation; RFU, relative fluorescence units. *$p < 0.05$. **$p < 0.01$.

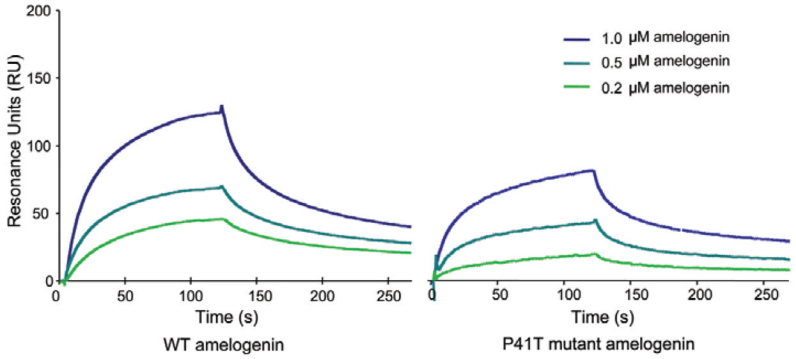

Figure 3.

Sensorgrams of surface plasmon resonance (SPR) analysis of the interactions between inactive E227A rhMMP20 and amelogenins (wild-type rh174 or P41T mutant). The binding affinity of the immobilized E227A rhMMP20 for wild-type rh174 amelogenin **(left panel)** was higher than that for the P41T mutant **(right panel)** at each concentration (0.2, 0.5, or 1 μM). Triplicate samples were performed at each amelogenin concentration, and the average values were used for construction of sensorgrams, from which K_{on} (on-rate constant), K_{off} (off-rate constant), K_a (affinity constant), and their variability were calculated (Table).

Table

Kinetic Values of rh174 and P41T Amelogenins Binding Affinity for E227A Inactive rhMMP20

	rh174 Wild-type Amelogenin** (mean ± SD, n = 3)	P41T Mutated Amelogenin (mean ± SD, n = 3)
K_{on} (1/Ms)	$6.45 \times 10^4 \pm 2.46 \times 10^4$	$1.87 \times 10^4 \pm 0.70 \times 10^4$ *
K_{off} (1/s)	$5.68 \times 10^{-3} \pm 0.90 \times 10^{-3}$	$5.86 \times 10^{-3} \pm 0.34 \times 10^{-3}$
K_a (1/M)	$1.19 \times 10^7 \pm 0.57 \times 10^7$	$3.23 \times 10^6 \pm 1.31 \times 10^6$ *

* $P < 0.05$

** rh174, wild-type recombinant full-length human amelogenin; P41T, mutated recombinant human amelogenin; E227A rhMMP20, recombinant human MMP20 with E227A mutation; K_{on}, on-rate constant; K_{off}, off-rate constant; K_a, affinity constant; SD, standard deviation.